Theoretical Study of Styrene (Methanol)$_n$ Clusters, $n = 1-9$. Comparison with Methanol Clusters

M. S. El-Shall,* D. Wright, Y. Ibrahim, and H. Mahmoud

Department of Chemistry, Virginia Commonwealth University, Richmond, Virginia 23284-2006

Received: February 10, 2003; In Final Form: May 15, 2003

The structures, energetics, and growth pattern of styrene (methanol)$_n$ clusters, (SM$_n$), with $n = 2-9$ are investigated using a search technique that employs Monte Carlo procedures. A 6−12−1 all-atom potential was developed that accurately reproduces the heat of vaporization, heat capacity, and density of liquid styrene. This potential, in conjunction with the OPLS potential for methanol, yields results strongly correlated with the experimental observations from our R2PI study of the SM$_n$ clusters. The progressive addition of methanol molecules to styrene leads to the formation of stable methanol clusters similar to those formed in the absence of styrene, with the exception of the SM$_3$ cluster where the lowest energy structure incorporates the methanol trimer as a hydrogen-bonded chain, rather than as the more stable cyclic structure of M$_3$. For the SM$_n$ clusters with $n = 4-9$, cyclic and branched cyclic methanol structures are found. In the clusters containing 5, 7, and 9 methanol molecules, the methanol subclusters are present on both sides of the plane of the styrene. The nonadditivity and size specificity of observed spectral shifts are explained through the use of a series of compact and expanded structures, with the interaction energy calculated between the styrene and the methanol subcluster (M$_n$). The results indicate that the spectral shifts correlate with the interaction energies between styrene and M$_n$ within the SM$_n$ clusters. The modeled cluster structures and simple energetic arguments provide a reasonably compelling picture of the spectral shifts associated with hydrogen bonding interaction among methanol molecules and between styrene and the methanol subclusters.

I. Introduction

The knowledge of the specific behavior of hydrogen bonding solvents in the presence of aromatic molecules is a key requirement for a molecular level understanding of many important processes in chemistry and biology such as the formation of clathrate hydrate and micelles, self-assembly, immiscibility of polar and nonpolar liquids, microphase separation, protein folding and biological activities.[1−5]

Fundamental insight into the hydrogen bonding−aromatic interactions can be obtained by studying binary clusters composed of a nonpolar aromatic and hydrogen-bonded molecules. These clusters constitute valuable models to study the role of intermolecular interactions, many-body interactions, and cooperative phenomena in the evolution of the rich equilibrium and dynamical behaviors known for condensed phase systems.[6−11]

Simulations of the thermodynamic, structural, and dynamic properties of *isolated* clusters have provided new insights into size effects in large finite systems and on the transition from molecular to macroscopic systems.[12−16] Much of the work has focused on rare gas and molecular clusters, but the simulation of hydrogen-bonded solvent clusters containing an aromatic solute has received little attention.[15−24] In the present paper, a search technique using Monte Carlo simulation procedures is used to help elucidate the structures and the nature of interactions within the styrene (methanol)$_n$ clusters, SM$_n$, with $n = 1-9$. For comparison, we also study the corresponding pure methanol clusters, M$_n$, $n = 2-9$.

Methanol is the smallest alcohol that has both hydrogen bonding and hydrophobic interactions. On the other hand, styrene contains both an unsaturated side chain and an aromatic ring linked by a covalent bond. Therefore, styrene (methanol)$_n$ clusters are good model systems to study hydrogen bonding interactions involving a single hydrogen donor configuration and an extended π-system.

The hydrogen bonding interaction in liquid and solid methanol is usually described in terms of a linear network winding in a zigzag manner.[25−32] In the solid state, methanol forms hydrogen-bonded chains with coordination number 2 and with adjacent chains pointing in opposite directions. The liquid structure can be described in terms of a competition between the close-packing of the methyl groups and the hydrogen bonding of the hydroxyl groups.[25] In the liquid state at room temperature, methanol exists in chains with two hydrogen bonds for each molecule. Rings and branched rings are the most common structures in the liquid, although arrangements with one terminating and three branching points are also present. Several questions remain regarding the exact structure of the liquid and the relative contributions of the cyclic and chain structures.[33−35]

Methanol clusters have already been the subject of both experimental and theoretical studies.[22−24,36−49] Minimum energy structures for small methanol clusters (M$_n$, with $n < 10$) have been obtained from empirical potentials, as well as ab initio and density functional calculations.[22−24,39,44−54] Monocyclic, semiplanar structures are found to persist at liquidlike temperatures for the smaller clusters, with bicyclic and polycyclic structures increasingly present in larger clusters. Large methanol clusters have been studied by molecular dynamics simulations.[55−57] Several properties such as the local density, electric potential, surface potential, and surface tension have been calculated using different potential models.[55−57]

Our main emphasis in this study is on how hydrogen bonding among methanol molecules is modified by the presence of a

10.1021/jp030176y CCC: $25.00
Published on Web 07/12/2003

styrene molecule, and whether it is possible to correlate the resonant 2-photon ionization (R2PI) spectral shifts of the SM_n clusters, relative to the styrene origin transition, with the interaction energies between styrene (S) and the methanol subcluster (M_n) in the SM_n clusters. For methanol we use the OPLS (optimized potential for liquid simulation) potential model.[58] This model reproduces the experimental temperature dependence of the second virial coefficients of methanol vapor with good accuracy, as well as several properties of liquid methanol.[22] For styrene, potential function parameters have been developed, and these are used in conjunction with the OPLS methanol parameters to obtain structures and interaction energies for various isomers of the SM_n clusters with $n = 1-9$.

In the remainder of this paper, section II gives computational details. section III presents a summary of our results for pure methanol clusters, describes and evaluates the new potential function for styrene, and investigates the structures and interaction energies of SM_n clusters. Section III also compares the size-dependence of properties in SM_n clusters to that in M_n clusters, and examines the strong correlations found between modeled and observed properties of SM_n clusters. Section IV summarizes the salient results of this work.

II. Pair Potential Calculations of Structures and Energies

Cluster interaction energies were calculated from site−site potentials of the form

$$\Delta e_{ab} = \sum_{i}^{\text{on a}}\sum_{j}^{\text{on b}}\left(\frac{q_i q_j e^2}{r_{ij}} + \frac{A_{ij}}{r_{ij}^{12}} - \frac{C_{ij}}{r_{ij}^{6}}\right) \quad (1)$$

where Δe_{ab} is the interaction energy between two molecules a and b, and the A_{ij} and C_{ij} can be expressed in terms of the Lennard-Jones σ's and ϵ's as $A_{ii} = 4\epsilon_i\sigma_i^{12}$ and $C_{ii} = 4\epsilon_i\sigma_i$,[6] and the combining rules $A_{ij} = (A_{ii}A_{jj})^{1/2}$ and $C_{ij} = (C_{ii}C_{jj})^{1/2}$ were used. The q_i are the partial charges assigned to each site and e is the magnitude of the electron charge.

For methanol, the 3-site OPLS potential was used, which treats the methyl group as a single site.[58] For the sites (O, CH_3, H) the σ's are (3.07, 3.775, 0), the ϵ's are (0.17, 0.207, 0), and the q's are (−0.700, 0.265, 0.435). The C−O bond length is 1.43 Å, the O−H bond length is 0.945 Å, and the COH angle is 108.5°. For styrene, a 16-site (all-atoms) model was developed that includes the internal rotation of the ethylene group, as described in a later section.

The total cluster configurational energy can be expressed as

$$\Delta E = \Delta E_C + \Delta E_{LJ} + \Delta E_S \quad (2)$$

where ΔE_C is the sum of all terms representing Coulomb interactions, ΔE_{LJ} is the sum of all Lennard-Jones terms, and ΔE_S is the intramolecular torsional energy of the styrene. Alternatively, the total energy can be expressed as

$$\Delta E = \Delta E_M + \Delta E_{S-M} + \Delta E_S \quad (3)$$

where ΔE_M is the sum of all terms involving methanol−methanol interactions, and ΔE_{S-M} the sum of all terms involving styrene−methanol interactions.

The software used for the Monte Carlo simulations was developed in our laboratory and has been used in several previous studies.[20,23,59] Many of the core routines were adapted from Jorgensen's MCLIQ (1990) program.[60]

Cluster structures and energies are obtained through the following simulation procedure. Monte Carlo simulations in the NVT ensemble are run for each cluster size using standard procedures, without truncation of the potential and at a temperature at which no evaporation is observed. At regular intervals during these simulations, the current cluster configuration is taken as an initial structure for a "quench" in which the cluster is settled into the underlying minimum on the potential surface. This is done by accepting only those small random displacements and rotations that lower the potential energy. Eventually a minimum is reached, and when 6000 consecutive trial configurations fail to find a structure of lower energy, the configuration is identified as a candidate for a minimum on the surface. Subsequently, in a separate calculation, each candidate is run at 10^{-12} K to confirm that a minimum has in fact been found and to be sure that the bottom of the well has been reached. For each cluster composition M_n and SM_n, 50−100 quenches were performed. Most minima were located numerous times.

TABLE 1: Total Cluster Energy (ΔE), the Contribution from the Electrostatic Terms Only (ΔE^C), the Energy of the Methanol Subcluster (ΔE_M), and the Interaction Energy between the Styrene and the Methanol Subcluster (ΔE_{S-M}) (OPLS (3-Site) Potential for Methanol, 16-Site Potential for Styrene, Energies in kcal/mol)

methanol			styrene−methanol				
n	$-\Delta E$	$-\Delta E^C$	n	$-\Delta E$	$-\Delta E^C$	$-\Delta E_M$	$-\Delta E_{S-M}$
2	6.88	7.85	1	4.87	3.31	0	4.88
3 (a)	17.60	20.63	2 (a)	13.29	11.74	6.47	6.84
3 (b)	15.15	17.08	2 (b)	13.11	11.97	6.55	6.57
4 (a)	29.95	34.97	3 (a)	22.89	21.93	14.57	8.34
4 (b)	24.50	27.49	3 (b)	22.87	21.77	14.52	8.36
			3 (c)	22.09	21.35	17.38	4.71
5 (a)	39.96	46.34					
5 (b)	37.16	41.15	4 (a)	35.31	35.55	29.79	5.53
5 (c)	33.56	36.86	4 (b)	35.25	35.53	29.77	5.49
6 (a)	49.11	56.77	5 (a)	46.46	47.56	39.78	6.68
6 (b)	48.94	55.96	5 (b)	46.24	47.52	39.78	6.46
6 (c)	42.71	46.40					
			6 (a)	54.04	53.65	47.39	6.66
7 (a)	57.11	62.15	6 (b)	53.79	54.28	47.15	6.64
7 (b)	56.60	62.32					
7 (c)	56.22	60.47	7 (a)	64.50	64.68	55.90	8.60
			7 (b)	64.12	64.51	55.70	8.42
8 (a)	68.44	76.14					
8 (b)	68.07	76.03	8 (a)	70.97	71.23	65.07	5.93
8 (c)	65.52	70.37	8 (a)	70.93	71.07	65.10	5.84
9 (a)	77.93	84.80	9 (a)	86.25	85.66	75.52	10.78
9 (b)	77.75	85.28	9 (b)	84.87	86.35	76.70	8.17
9 (c)	72.31	77.04					

A measure of cluster radius is given by the root-mean-square distance between the molecules, given by[61]

$$R_n = \left\langle\left(\sum_{i}^{n-1}\sum_{j>i}^{n}\frac{r_{ij}^{\,2}}{n(n-1)}\right)^{1/2}\right\rangle \quad (4)$$

The intermolecular distances, r_{ij}, were taken as the separations of the molecular centers-of-mass, and n is the number of molecules in the cluster. This is useful for accessing the degree of compactness of clusters.

III. Results and Discussion

A. Methanol Clusters, M_n, $n = 2-9$. The interaction energies of some of the more stable structures of pure methanol clusters are summarized in Table 1. Figure 1a displays the cluster total energy per molecule ($\Delta E/n$) and the Coulomb contribution per molecule ($\Delta E_C/n$) as functions of n. For the small methanol clusters of this study, the entire binding energy arises from the

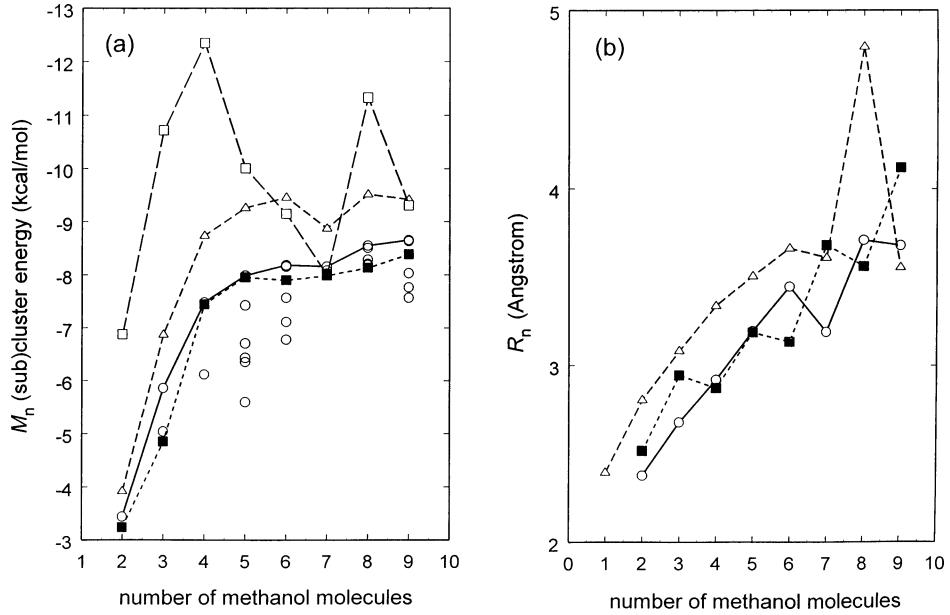

Figure 1. (a) Energetics of the pure methanol clusters and in the presence of styrene. The symbols used are (○−○) total energy per molecule; (△) coulomb terms only, per molecule; (□) total energy (n) − total energy (n − 1); (○, without connecting line) total energy per molecule, other isomers; (■) total energy, per methanol molecule, styrene present. (b) Root-mean-square distances between the molecular centers of mass for pure methanol clusters (○), methanol only with styrene present (■), and methanol-to-styrene only (△).

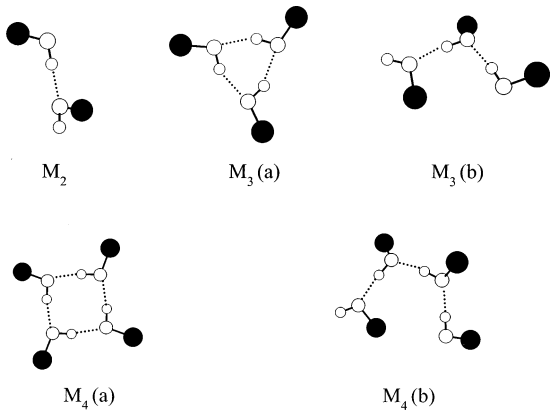

Figure 2. Lowest energy structures of methanol clusters (M_n) with n = 2−4.

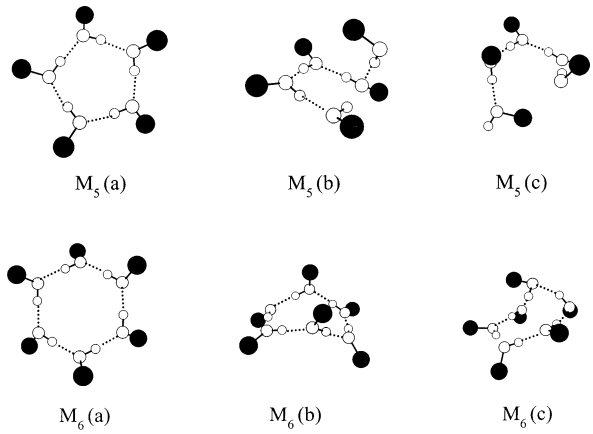

Figure 3. Lowest energy structures of methanol clusters (M_n) with n = 5, 6.

Coulomb terms and the LJ terms are net positive. With the OPLS potential, the LJ terms become net attractive only for $n > 30$. There is a rapid decrease in $\Delta E/n$ with n up to $n = 4$, followed by relatively small changes until a notable decrease at $n = 8$. The incremental interaction energies [$\Delta E_n - \Delta E_{n-1}$] vs n show pronounced maxima (most negative) for the tetramer and octamer.

Figure 1b displays the variation of R_n with n for methanol clusters in the absence and presence of styrene. Values of R_n were also computed using only the methanol-to-styrene distances in the SM_n clusters and are also shown in Figure 1b. The trends observed in R_n will be discussed in section E, following discussion of the structures of these clusters.

Selected structures for the methanol clusters are shown in Figures 2−6. For each cluster size with $n > 2$, the two isomers lowest in energy are always included. The lowest energy structure of the methanol dimer has an almost linear O−H- - -O bond with the O−H- - -O−H angle = 178.6°. The lowest energy structures of the trimer [M_3(a)] and tetramer [M_4(a)] correspond to planar cyclic structures with C_{3h} and C_{4h} symmetry, as shown in Figure 2. The M_3(a) cyclic structure has three equivalent H-bonds (1.85 Å) with an O- - -H−O angle of 152.8°. The H-bond in the M_4(a) structure (1.75 Å) is shorter than in the M_3(a) structure, and the O−H- - -O angle is 167.5°. The second-lowest energy isomer for the trimer [M_3(b)] and tetramer [M_4(b)] corresponds to a chain structure (shown in Figure 2) at 14% and 18% higher energy, respectively, than the corresponding cyclic structure.

The lowest energy pentamer [M_5(a)] has a semiplanar cyclic structure with an H-bond length of 1.74 Å and O−H- - -O angles near 174° (shown in Figure 3). The second- and third-lowest energy isomers [M_5(b) and M_5(c)] correspond to a branched tetramer and a chain structure at 7% and 16% higher energy, respectively, than the M_5(a) cyclic structure. The two lowest energy isomers of the hexamer correspond to a ring with S_6 symmetry [M_6(a)] and a chain structure [M_6(b)], respectively, as shown in Figure 3. Also shown in Figure 3 is the higher energy isomer [M_6(c)], which has a lower symmetry ring structure. The cyclic structure M_6(c) resembles the well-known "*book*" structure found as one of the most stable water hexamer structures.[62,63]

The three lowest energy structures of M_7 can be described as either a branched cyclic hexamer [M_7(a)], or a branched cyclic pentamer [M_7(b) and M_7(c)], as shown in Figure 4. The

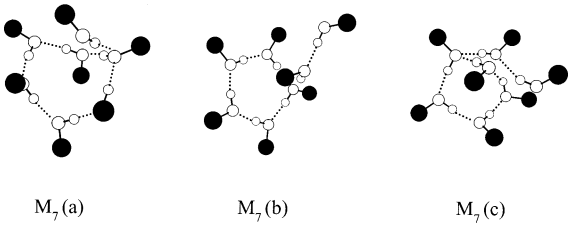

Figure 4. Lowest energy isomers of (methanol)$_7$, M_7.

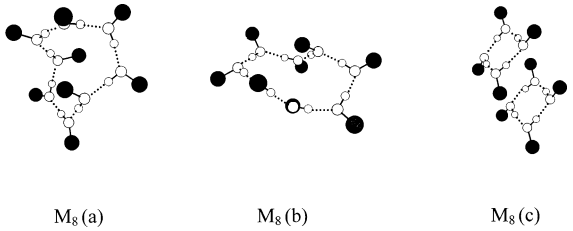

Figure 5. Lowest energy isomers of (methanol)$_8$, M_8.

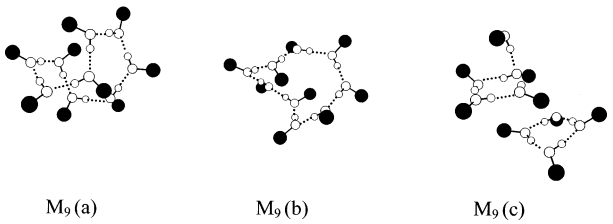

Figure 6. Lowest energy isomers of (methanol)$_9$, M_9.

interaction energies of the M_7(b) and M_7(c) isomers are within 2% or less of the interaction energy of the most stable isomer M_7(a). For M_8, the two most stable structures are semiplanar rings [M_8(a) and M_8(b)] with M_8(b) exhibiting a larger and more open ring, as shown in Figure 5. Another interesting octamer structure was also found [M_8(c)], consisting of two cyclic tetramers without H-bonds between them, and at only 4.3% higher energy than the lowest isomer M_8(a).

The lowest energy isomer of the M_9 cluster, [M_9(a)] (shown in Figure 6), can be described as a twisted cyclic structure consisting of a tetramer and a pentamer as upper and lower parts, respectively, of a fully cyclic structure that traces out like a "figure 8". The second isomer [M_9(b)] appears as a more open cyclic structure, and the third isomer [M_9(c)] consists of a cyclic tetramer and a branched tetramer (4+1) without H-bond bridges between the two substructures.

The cluster energies given in Table 1 indicate that the interaction energies of the lowest energy cyclic trimer, tetramer, pentamer, and hexamer are −17.6, −30.0, −40.0, and −49.1 kcal/mol, respectively. The corresponding interaction energies per H-bond are −5.9, −7.5, −8.0, and −8.2 kcal/mol for the trimer, tetramer, pentamer, and hexamer, respectively. A similar trend has been observed in the density functional calculations of methanol clusters, where the interaction energies per H-bond were found to be −6.1, −8.2, and −8.6 kcal/mol in the cyclic trimer, tetramer, and pentamer, respectively.[49]

The structures of the methanol clusters obtained using the OPLS potential generally agree with the results obtained by Buck et al. using a potential based on the methanol wave functions.[24] The main differences are the lowest energy structures of the trimer and tetramer where lower symmetry ring structures were found as reported in ref 24. It should be noted that ab initio and density functional calculations predict the global minimum of the methanol trimer to be a cyclic structure with two methyl groups on one side of the O−O−O plane and the third one on the other side.[48,49] However, in the ab initio study the structure having the three methyl groups on the same side of the O−O−O plane (similar to the lowest energy structure found in the present study) was found to lie only 0.8 kcal/mol above the global minimum.[48]

TABLE 2: Partial Charge Assignments for the Styrene Potential Function[a]

site	q_i	site	q_i	site	q_i	site	q_i
1	−0.0071	5	−0.1157	9	0.1203	13	0.1185
2	−0.1193	6	−0.1281	10	0.1197	14	0.1092
3	−0.1179	7	−0.0678	11	0.1194	15	0.1054
4	−0.1216	8	−0.2364	12	0.1199	16	0.1013

[a] The charges are numbered as shown in Figure 7 (first panel).

B. Potential Function for Styrene. An all-atom potential function was developed for styrene using the all-atom (12-site) OPLS potential for benzene as a departure point, and a derivative of W. L. Jorgensen's MCLIQ (1990) program for liquid simulations.[60] As in the OPLS benzene potential, all carbon−carbon bond lengths were set to 1.4 Å, all carbon−hydrogen bond lengths set to 1.08 Å, all bond angles set to 120°, and the Lennard-Jones parameters (σ, ϵ) were set to (3.55, 0.07) for each carbon and to (2.42, 0.03) for each hydrogen. This leaves only the partial charges q_i to be assigned for styrene. Trial values for the q_i were taken from ab initio (HF/6-31G** basis set) calculations for the styrene monomer.[64] The q_i were then optimized using results from simulations of liquid styrene in the NPT ensemble at 25° C and 1 atm. Standard MC procedures such as Metropolis sampling, a cubical cell with 128 monomers, periodic boundary conditions, and a cutoff correction to the energy were used. The production run of 9.5×10^6 configurations was made after more than 4×10^6 configurations of equilibration. The intramolecular torsional energy is represented using[65]

$$V(\varphi) = (V_2/2)(1 - \cos 2\varphi) \tag{5}$$

where $V_2 = 2.20$ kcal/mol[66] and φ is the angle between the plane of the phenyl ring and the plane of the ethylene group.

In the optimization of the q_i, a single scale factor λ was used to scale all q_i, and with modest scaling ($\lambda = 0.80$) the resultant potential function well reproduced key properties of liquid styrene. The optimized charges are given in Table 2.

For styrene, the enthalpy of vaporization[60] to the ideal gas and to the real gas are the same and the enthalpy departure function, $H° - H^g_{sat}$, is nearly zero, because the temperature of the simulations (25 °C) is far below the boiling point of styrene (146 °C), and

$$\begin{aligned}\Delta H_{vap} &= E_{total}(g) - E_{total}(l) + RT \\ &= E_{intra}(g) - E_{inter}(l) - E_{intra}(l) + RT\end{aligned} \tag{6}$$

$E_{intra}(g)$ is computed for a Boltzmann distribution for the torsional potential with a value of 0.36 kcal/mol, and from the MC simulation $E_{intra}(l)$ is 0.287 ± 0.002 kcal/mol and $E_{inter}(l)$ is −9.88 ± 0.02 kcal/mol. Our value for $E_{intra}(l)$ matches that obtained by Jorgensen for anisole, as OPLS anisole has a torsional potential identical to that used here for styrene. The calculated value for styrene is thus 10.54 ± 0.02 kcal/mol, in excellent agreement with the experimental value of 10.50 ± 0.10 kcal/mol.[66]

The constant pressure heat capacity for the liquid, $C_P(l)$, is estimated as a contribution from the fluctuation in the intermolecular energy, C_P^{inter}, plus an intramolecular term taken as the ideal gas heat capacity, $C_P°(g)$, less R, the gas constant.[60]

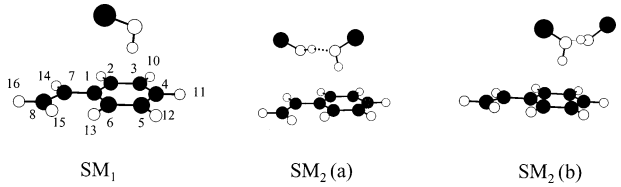

Figure 7. Lowest energy structures of styrene (methanol)$_n$ clusters (SM$_n$) with $n = 1, 2$.

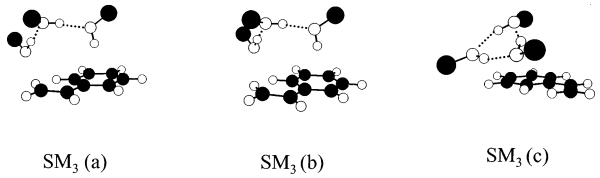

Figure 8. Lowest energy structures of styrene (methanol)$_3$ cluster (SM$_3$).

From the simulation, C_P^{inter} is 16.97 ± 1.44 cal/(mol K), and with $C_P°$(g) as 28.726 cal/(mol K),[67] the estimated C_P(l) is 43.71 ± 1.44 cal/(mol K). This is in excellent agreement with the experimental value of 43.7 ± 0.1 cal/)mol K).[66,68,69]

The simulated liquid density is 0.9141 ± 0.0012 g/cm^3, which differs by 1.4% from the experimental value of 0.9018 g/cm^3.[70] In the large set of OPLS potential functions, simulated results for the enthalpy of vaporization and liquid density are typically within 1−2%. For the liquid alcohols, the average error in the liquid density is 1.8%[58] and is of the same magnitude as obtained here for styrene.

It should be noted that the scaled charges shown in Table 2 are not symmetric with respect to flipping of the vinyl group. Symmetrizing the charges to make both ortho hydrogens equivalent resulted in slight modifications of the charges [3.5% (ortho C's), 0.75% (ortho H's), 0.94% (meta C's), or 0.083% (meta H's)]. Repeating the simulation of liquid styrene with symmetrized charges changed the liquid properties as follows: E_{total} (0.3%), E_{inter} (0.4%), E_{intra} (3.6%), C_P (6.7%), C_P^{inter} (17%), density (0.20%). The properties computed from fluctuations, the liquid heat capacity, the isothermal compressibility, and the coefficient of thermal expansion, all decreased upon symmetrizing the potential, which seems reasonable. The symmetrized potential gave slightly more accurate values for the enthalpy of vaporization and the liquid density (both potentials do quite well on these properties), but gave a poorer value for the liquid heat capacity. Although both simulations consisted of 9.5 × 10^6 configurations, longer simulations are perhaps needed for adequate convergence of the heat capacity. The average errors in the properties of liquid styrene calculated using the parameters given in Table 2 in comparison with experimental data, are comparable to the errors reported using the OPLS-AA force field for organic molecules recently developed by Jorgensen.[71]

C. Styrene (Methanol)$_n$ Clusters, SM$_n$, $n = 1-9$. The lowest energy structure found for the SM cluster places the methanol above the phenyl ring of styrene with the hydrogen of the OH group pointing toward the center of the ring, as shown in Figure 7. This is a direct result of the columbic attraction between H and the π-system. The structure is similar to that of the benzene (methanol) cluster obtained using OPLS potential functions.[72]

The two lowest energy isomers [SM$_2$(a) and SM$_2$(b)] of the SM$_2$ cluster are shown in Figure 7. The difference in the binding energies between the two structures is only 0.2 kcal/mol. It is interesting to note that the hydrogen bond length in SM$_2$(a) or SM$_2$(b) (1.78 A°) is almost the same as in the isolated M$_2$ structure (1.79 A°), but the O−H- - -O geometry is less linear in SM$_2$(a) or SM$_2$(b) (172°) than in the isolated M$_2$ structure (179°). Also, the energy of M$_2$ in SM$_2$(a) or SM$_2$(b) (−6.5 or −6.6 kcal/mol, respectively) is slightly higher than in isolated M$_2$ (−6.9 kcal/mol). In SM$_2$(a) the two methanol molecules show interactions with both the phenyl ring and the ethylene chain, whereas in SM$_2$(b) most of the interactions are with the phenyl ring.

The SM$_2$(a) structure is a good candidate for the assigned SM$_2$−II isomer (see preceding paper),[73] which shows a small blue shift and little fragmentation to the SM$^+$ channel following ionization consistent with the absence of a single H-bonding interaction to the styrene ring. The second calculated structure SM$_2$(b) matches the observed behavior of the assigned SM$_2$−I isomer, which shows a strong blue shift of 84 cm^{-1} and strong fragmentations to the SM$^+$ channel following the ionization of the cluster.

It is interesting to find that the lowest energy isomer of the SM$_3$ cluster incorporates the methanol trimer as an H-bonded chain rather than as the cyclic structure found in the isolated M$_3$ global minimum. The structure of M$_3$ in SM$_3$(a), shown in Figure 8, is actually similar to the structure of the second lowest energy isomer of isolated M$_3$. This is also evident by comparing the interaction energy of M$_3$ in SM$_3$(a) (−14.6 kcal/mol) with that of M$_3$(b) (−15.2 kcal/mol). Another structure of the SM$_3$ cluster, shown as SM$_3$(b) in Figure 8, has an energy similar to SM$_3$(a), but a different orientation of the M$_3$ chain with respect to styrene. Another isomer [SM$_3$(c)] was also found, as shown in Figure 8, but at 3.5% higher energy than SM$_3$(a). Interestingly, this isomer incorporates M$_3$ as a cycle similar to the lowest energy structure of the isolated methanol trimer. The energy of the methanol cyclic trimer in SM$_3$(c) (−17.4 kcal/mol) is close to that of isolated M$_3$ (−17.6 kcal/mol). However, unlike the symmetric ring of M$_3$ with three equivalent H-bonds, the M$_3$ ring in SM$_3$(c) has one elongated H-bond (O$_1$−H- - -O$_3$, 1.92 Å) and two shorter equivalent H-bonds (1.83 Å).

It is important to note that the interaction energy between styrene and the methanol trimer is stronger in SM$_3$(a) (−8.3 kcal/mol) than in SM$_3$(c) (−4.7 kcal/mol). This indicates that the interaction of styrene with the methanol trimer chain provides extra stabilization over that resulting from the cyclization of the methanol trimer. This is consistent with previous studies of benzene (methanol)$_n$ clusters, where the methanol trimer was found to adopt a chain rather than a ring structure in the presence of benzene.[49] The structure SM$_3$ (a) is a good candidate for the assigned SM$_3$−I isomer, which exhibits a large blue shift and shows very strong fragmentation to the SM$_2$ channel following ionization, consistent with H-bonding interaction. The structure of SM$_3$ (c) is in agreement with the observation of the SM$_3$−II isomer, which has a small blue shift and shows little fragmentation to the SM$_2$ channel following ionization.

The two lowest energy isomers found for the SM$_4$ cluster [SM$_4$(a) and SM$_4$(b)] are shown in Figure 9. Both isomers contain highly symmetric cyclic M$_4$ subclusters and differ mostly in the orientation of the M$_4$ ring with respect to styrene. Again, the interaction energy of the M$_4$ ring in the SM$_4$ clusters (−29.8 kcal/mol) is nearly similar to that of the isolated cyclic tetramer (−30.0 kcal/mol). The exceptional stability of the methanol tetramer ring results in a relatively weak interaction with styrene (−5.5 kcal/mol)—most of the SM$_4$ interaction energy resides within the methanol subcluster rather than in the styrene−M$_4$ attachment. This is clearly evident in the styrene-to-methanol subcluster interaction energies ($\Delta E_{\text{S-M}}$) for SM$_3$(a) and SM$_4$(a). SM$_3$(a) incorporates the less stable chain (rather than cyclic) M$_3$ subcluster and has an $\Delta E_{\text{S-M}}$ of −8.3 kcal/mol,

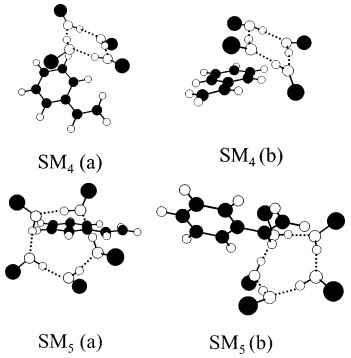

Figure 9. Lowest -energy structures of styrene (methanol)$_n$ clusters (SM_n) with $n = 4, 5$.

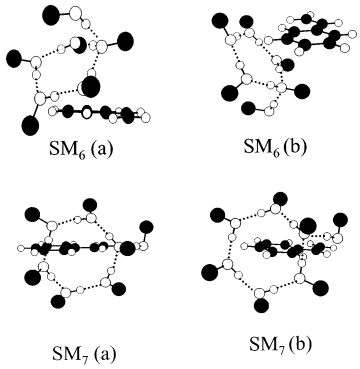

Figure 10. Lowest energy structures of styrene (methanol)$_n$ clusters (SM_n) with $n = 6, 7$.

whereas SM_4(a) incorporates the most stable M_4 subcluster and has an ΔE_{S-M} of only -5.5 kcal/mol, as shown in Table 1.

The two nearly degenerate structures of the SM_4 cluster, SM_4-(a) and SM_4(b) are excellent candidates for the single isomer observed for this cluster. This cluster shows a remarkable switch in the spectral shift from blue to red, in full agreement with the formation of a methanol tetramer ring where the interaction with styrene becomes predominantly dispersive. Dispersion interactions are usually associated with red spectral shifts in clusters containing an aromatic chromophore.[74]

The two lowest energy isomers of the SM_5 clusters are shown in Figure 9. Both SM_5 structures show methanol pentamer rings similar to (but less symmetric than) the isolated cyclic pentamer, and these are the first clusters to show the methanol subcluster present on both sides of the plane of the phenyl ring of styrene. These structures are in agreement with the observation of two red-shifted isomers for each of the SM_5 and SM_6 clusters. For the SM_6 cluster, the two lowest energy isomers (shown in Figure 10) do not incorporate the methanol hexamer in its most stable isolated structure. In both SM_6(a) and SM_6(b), the methanol subcluster is present as a cyclic pentamer with an attached monomer (branched structure), rather than the hexagonal structure found for the isolated hexamer.

The two lowest energy isomers of SM_7 are shown in Figure 10. Both structures of SM_7 show branched cyclic methanol hexamers resembling the lowest energy structures of the isolated M_7. Also, similar to SM_5, but unlike SM_6, the methanol subcluster in SM_7 lies on both sides of the plane of the styrene ring.

The structures of the two isomers of SM_8 (displayed in Figure 11) show a pair of cyclic methanol tetramers without H-bonds between them. Interestingly, both tetramers lie entirely on one side of the plane of the styrene phenyl ring. These isomers show the methanol octamer in the same structure as M_8(c), which

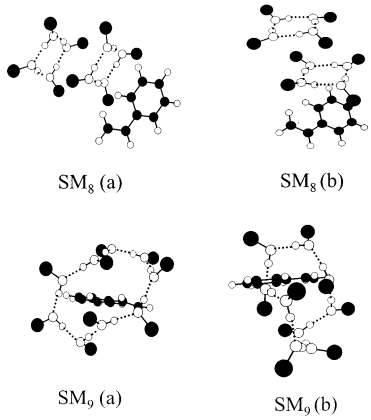

Figure 11. Lowest -energy structures of styrene (methanol)$_n$ clusters (SM_n) with $n = 8, 9$.

has an energy 4.3% higher than that of the most stable isolated methanol octamer [M_8(a)]. The lowest energy isomer [SM_8(a)] exhibits a smaller styrene-to-methanol interaction energy ($\Delta E_{S-M} = -5.9$ kcal/mol) than the lowest energy isomers of the SM_5-SM_7 clusters [$\Delta E_{S-M} = -6.7$, -6.7, and -8.6 kcal/mol, for SM_5(a), SM_6(a), and SM_7(a), respectively]. This indicates that most of the stability of the SM_8 cluster is due to the large stability of the methanol octamer in the "twin-cyclic tetramer" configuration.

The two SM_9 isomers (displayed in Figure 11) show large monocyclic methanol subclusters that span both sides of the styrene phenyl plane. The sudden increase in ΔE_{S-M} (-10.8 kcal/mol) in SM_9(a) is probably due to efficient wrapping of the M_9 subcluster around both sides of the styrene plane.

It should be noted that upon repeating the simulation of the SM cluster with the symmetrized styrene potential, the cluster properties changed as follows: E_{total} (0.010%), E_C (0.11%), E_{LJ} (0.063%), E_{intra} (5.1%), R_n (0.025%), and the cluster structure was (visually) indistinguishable from that obtained with the (unsymmetrized) potential with the parameters given in Table 2. This result indicates that for the energetics and structures of small gas-phase clusters at 0 K, the use of a symmetrized potential gives results similar to those of the potential utilizing charges as obtained from ab initio calculations.

D. Growth Patterns and Correlation with Spectral Shifts. The perturbation of the structures of the most stable methanol clusters caused by the presence of styrene can be examined using the root-mean-square distance between the molecules (R_n) given by eq 4, which provides a measure of relative cluster radius and is useful in assessing the relative degree of compactness among a series of clusters. The plot in Figure 1b of R_n vs n for the methanol subclusters in SM_n shows an interesting even-odd alternation, which is not present in the isolated methanol clusters. For $n = 4$, 6, and 8, R_n for the methanol cluster is smaller when the styrene is present, yet for $n = 3$, 7, and 9, R_n is larger when the styrene is present. For $n = 5$, the R_n values are nearly equal in the presence and absence of styrene. This pattern can be explained by comparing the structures of the lowest energy isomers of SM_4-SM_9, which are shown in Figures 12 and 13. It is clear that in the SM_n clusters, the even-n methanol subclusters lie entirely on one side of the plane of the styrene phenyl ring, as shown in Figure 12, whereas the odd-n subclusters are present on both sides of this plane to about equal extents (shown in Figure 13). This indicates that for $n = 4$, 6, and 8, the methanol subcluster is more compact than the isolated methanol cluster of the same size. These compact clusters can optimize all intermolecular interactions with the

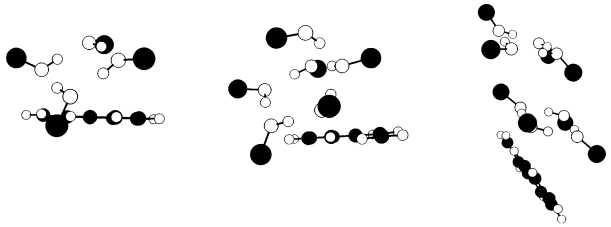

Figure 12. Lowest energy isomers of the SM_n clusters with n even (4, 6, and 8). Note that the methanol subcluster is present on one side of the styrene plane.

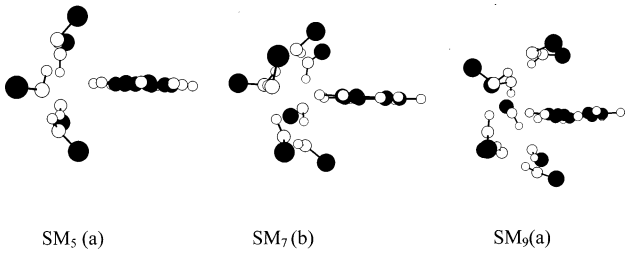

Figure 13. Lowest energy isomers of the SM_n clusters with n odd (5, 7, and 9). Note that the methanol subcluster is present on both sides of the styrene molecular plane.

styrene with little hindrance; hence a red shift in the cluster's origin is observed. The opposite trend is observed for the clusters with 7 and 9 methanol molecules, as these expanded clusters tend to rap around both sides of the styrene molecules.

Figure 14 displays plots of interaction energy ΔE_{S-M} (the styrene-to-methanol interaction energy) as a function of n for the SM_n clusters, as well as the observed spectral shifts reported in the preceding paper.[73] The similarity between the two trends is remarkable! In particular, the largest red shift and the smallest styrene-to-methanol interaction energy (next to the SM cluster) are both observed in SM_4. Similarly, the red shift observed for the SM_8 cluster correlates with the styrene-to-methanol interaction energy calculated for this cluster. Also, the clusters that exhibit maxima in the magnitude of the blue spectral shift relative to the isolated styrene molecule (SM_9, SM_7, and SM_3) also exhibit maxima in magnitude of ΔE_{S-M}.

Because the calculated ΔE_{S-M} pertains to the cluster ground state, the strong correlation between styrene-to-methanol interaction and spectral shift suggests that these shifts are mainly dependent on the ground-state styrene-to-methanol interaction.

IV. Summary and Conclusions

In the present work, new potential function parameters have been reported for styrene that yield results in general accord with the properties of liquid styrene. This potential, in conjunction with the OPLS potential for methanol, yields results strongly correlated with the experimental observations of the R2PI study of styrene−(methanol)$_n$ clusters. The progressive addition of methanol molecules to styrene leads to the formation of stable methanol clusters similar to those of pure isolated methanol clusters, with the exception of the styrene (methanol)$_3$ cluster. In this case, the lowest energy structure does not incorporate

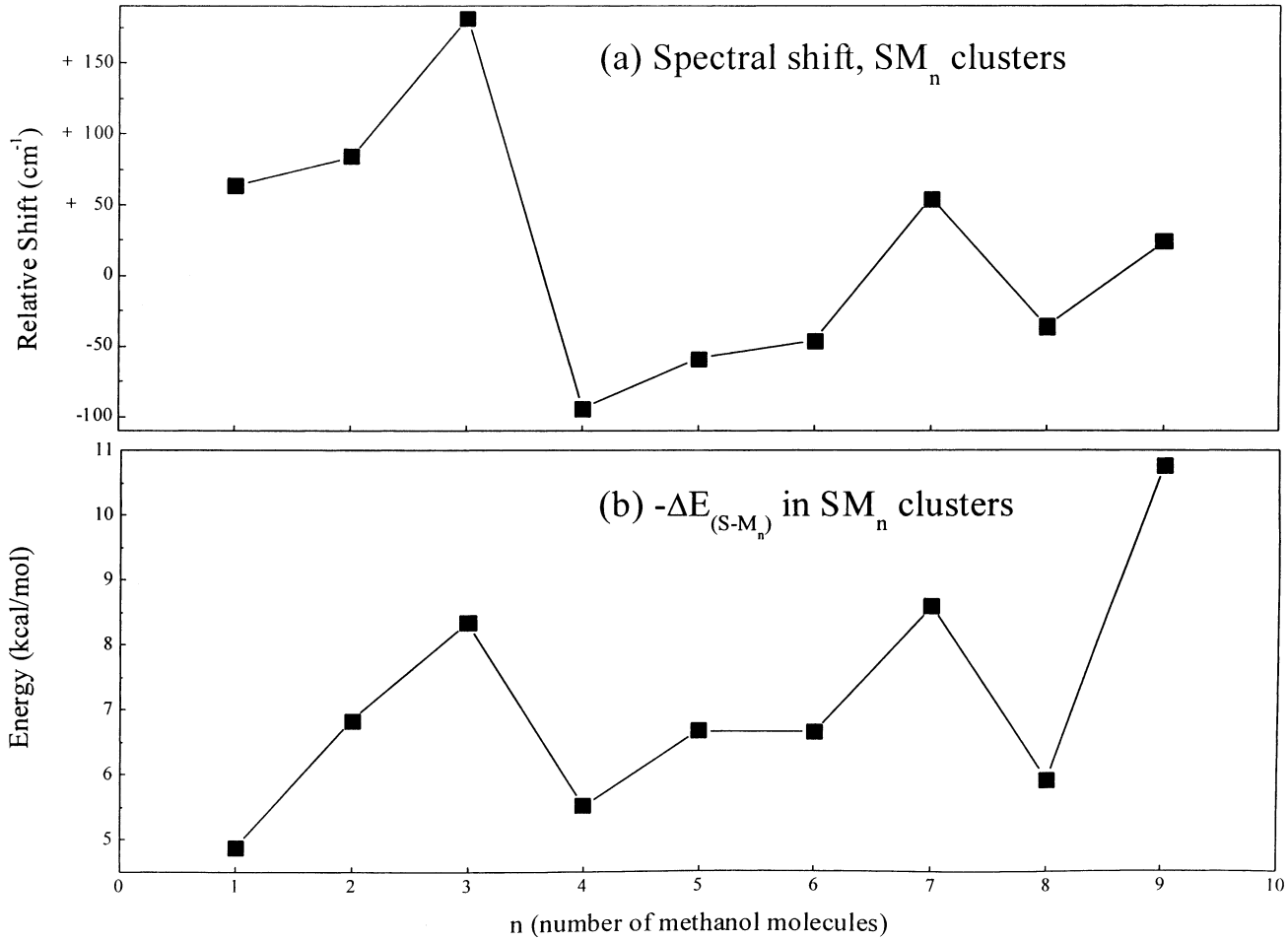

Figure 14. (a) Experimental spectral shifts of the SM_n cluster origins relative to the 0_0^0 origin of isolated styrene molecule (see ref 73). (b) Calculated interaction energies between styrene (S) and the methanol subcluster (M_n) in the lowest energy isomers of the SM_n clusters.

the methanol trimer as a cyclic structure, but as a hydrogen-bonded chain. In all the larger sizes ($n = 4-9$), cyclic methanol subclusters have been found in the styrene (methanol)$_n$ clusters.

We have observed three computational quantities or structural features that correlate with the observed spectral shifts in small SM_n clusters: (1) the S-to-M_n subcluster interaction energies, (2) the shift in R_n for the M_n clusters when styrene is present, and (3) the even−odd alternation in how the M_n subclusters are positioned with respect to the plane of the styrene ring. The nonadditivity and size specificity of the observed spectral shifts is explained through the use of a series of compact and expanded structures, with the interaction energy calculated between the styrene and the methanol subcluster. The correlation between the experimental spectral shifts and the solute−solvent interaction energies in the ground states of the clusters (and the other correlations as well) support the validity of using potential functions developed using properties of the bulk liquids to study small clusters generally, and in particular they build confidence in the styrene potential function presented in this work.

Acknowledgment. We gratefully acknowledge financial support from NSF Grant No. CHE 9816536. Acknowledgment is also made to the donors of the Petroleum Research Fund, administered by the American Chemical Society, for the partial support of this research. We thank W. L. Jorgensen for making his MCLIQ (1990) program available for our use.

References and Notes

(1) Jeffrey, J. A.; Sanger, W. *Hydrogen Bonding in Biological Structures*; Springer: Verlag: Berlin, 1991.

(2) Pimentel, G. C.; McClellan, A. C. In *The Hydrogen Bond*; Pauling, L., Ed.; Freeman: San Francisco, 1960.

(3) Scheiner, S. *Hydrogen Bonding: A Theoretical Perspective*; University Press: Oxford, 1977.

(4) Tanford, C. *The Hydrophobic Effect: Formation of Micelles and Biological Membranes*; Wiley: New York, 1980.

(5) Privalov, P.; Gill, S. S. J. *Adv. Protein Chem.* **1988**, *40*, 191.

(6) Curtiss, L. A.; Blander, M. *Chem. Rev.* **1988**, *88*, 827. Hobza, P.; Zahradnik, R. *Chem. Rev.* **1988**, *88*, 871. Buckingham, A. D.; Fowler, P. W.; Hutson, J. M. *Chem. Rev.* **1988**, *88*, 963.

(7) Atwood, J. L.; Hamada, F.; Robinson, K. D.; Orr, G. W.; Vincent, R. L. *Nature* **1992**, *349*, 683.

(8) Rodham, D. A.; Suzuki, S.; Suenram, R. D.; Lovas, F. J.; Dasgupta, S.; Goddard, W. A., III.; Blake, G. A. *Nature* **1993**, *362*, 735.

(9) Kim, K. S.; Lee, J. Y.; Lee, S. J.; Ha, T. K.; Kim, D. H. *J. Am. Chem. Soc.* **1994**, *116*, 7399.

(10) Gregory, J. K.; Clary, D. C. *J. Phys. Chem.* **1996**, *100*, 18014.

(11) Zwier, T. S. *Annu. Rev. Phys. Chem.* **1996**, *47*, 205.

(12) Lee, J. K.; Barker, J. A.; Abraham, F. F. *J. Chem. Phys.* **1973**, *58*, 3166.

(13) Kristensen, W. D.; Jensen, E. J.; Cotterill, R. M. J. *J. Chem. Phys.* **1974**, *60*, 4161.

(14) Etters, R. D.; Kaelberer, J. B. *Phys. Rev. A* **1975**, *11*, 1068.

(15) Berry, R. S.; Beck, T. L.; Davies, H. L.; Jellinek, J. *Adv. Chem. Phys.* **1988**, *70*, 74.

(16) Jellinek, J.; Beck, T. L.; Berry, R. S. *J. Chem. Phys.* **1986**, *84*, 2783.

(17) Del Mistro, R. S.; Stace, A. *J. Chem. Phys. Lett.* **1990**, *171*, 381.

(18) Dulles, F. J.; Bartell, L. S. *J. Phys. Chem.* **1995**, *99*, 17100.

(19) Al-Mubarak, A. S.; Del Mistro, G.; Lethbridge, P. G.; Abdul-Sattar, N. Y.; Stace, A. J. *Discuss. Faraday Soc.* **1988**, *86*, 209.

(20) Wright, D.; El-Shall, M. S. *J. Chem. Phys.* **1994**, *100*, 379.

(21) Wales, D. J.; Ohmine, I. *J. Chem. Phys.* **1993**, *98*, 7245, 7257.

(22) Buck, U.; Schmidt, B. *J. Chem. Phys.* **1993**, *98*, 9410.

(23) Wright, D.; El-Shall, M. S. *J. Chem. Phys.* **1996**, *105*, 11199.

(24) Buck, U.; Siebers, J. G.; Wheatley, R. J. *J. Chem. Phys.* **1988**, *108*, 20.

(25) Narten, A. H.; Habenschuss, A. J. *J. Chem. Phys.* **1984**, *80*, 3387.

(26) Steytler, D. C.; Dore, J. C.; Montague, D. C. *J. Non-Cryst. Solids* **1985**, *74*, 303.

(27) Jorgensen, W. L. *J. Am. Chem. Soc.* **1980**, *102*, 543. Jorgensen, W. L. *J. Am. Chem. Soc.* **1981**, *103*, 341.

(28) Vij, J. K.; Reid, C. J.; Evans, M. W. *Mol. Phys.* **1983**, *50*, 935.

(29) Haughney, M.; Ferrario, M.; McDonald, I. R. *J. Phys. Chem.* **1987**, *91*, 4934.

(30) Hawlicka, E.; Palinkas, G.; Heinzinger, K. *Chem. Phys. Lett.* **1989**, *154*, 225.

(31) Svishchev, I. M.; Kusalik, P. G. *J. Chem. Phys.* **1994**, *100*, 5165.

(32) Bulgarevich, D. S.; Otake, K.; Sako, T.; Sugeta, T.; Takebayashi, Y.; Kamizawa, C.; Shintani, D.; Negishi, A.; Tsurumi, C. *J. Chem. Phys.* **2002**, *116*, 1995.

(33) Sarkar, S.; Joarder, R. N. *J. Chem. Phys.* **1993**, *99*, 2032.

(34) Shilov, I. Yu.; Rode, B. M.; Durov, V. A. *Chem. Phys.* **1999**, *241*, 75.

(35) Bako, I.; Jedlovszky, P.; Palinkas, G. *J. Mol. Liq.* **2000**, *87*, 243.

(36) Huisken, F.; Stemmler, M. *Chem. Phys. Lett.* **1988**, *144*, 391.

(37) Huisken, F.; Kulcke, A.; Laush, C.; Lisy, J. M. *J. Chem. Phys.* **1991**, *95*, 3924.

(38) Pugliano, N.; Saykally, R. J. *Science* **1992**, *257*, 1937.

(39) Anwander, E. H. S.; Probst, M. M.; Rode, B. M. *Chem. Phys.* **1992**, *166*, 341.

(40) Buck, U.; Schmidt, B.; Siebers, J. G. *J. Chem. Phys.* **1993**, *99*, 9428.

(41) Liu, K.; Loeser, J. G.; Elrod, M. J.; Host, B. C.; Rzepiela, J. A.; Pugliano, N.; Saykally, R. J. *J. Am. Chem. Soc.* **1994**, *116*, 3507.

(42) Buck, U.; Ettischer, I. *J. Chem. Phys.* **1994**, *100*, 6974.

(43) Liu, K.; Elrod, M. J.; Loeser, J. G.; Cruzan, J. D.; Pugliano, N.; Brown, M. G.; Rzepio, J.; Saykally, R. J. *Faraday Discuss.* **1994**, *97*, 35.

(44) Mo, O.; Yanez, M.; Elguero, J. *J. Mol. Struct.* **1994**, *314*, 73.

(45) Williams, R. W.; Cheh, J. L.; Lowrey, A. H.; Weir, A. F. *J. Phys. Chem.* **1995**, *99*, 5299.

(46) Bleiber, A.; Sauer, J. *Chem. Phys. Lett.* **1995**, *238*, 243.

(47) Huisken, F.; Kaloudis, M.; Koch, M.; Werhahn, O. *J. Chem. Phys.* **1996**, *105*, 8965.

(48) Mo, O.; Yanez, M.; Elguero, J. *J. Chem. Phys.* **1997**, *107*, 3592.

(49) Hgemeister, F. C.; Gruenloh, C. J.; Zwier, T. S. *J. Phys. Chem. A* **1998**, *102*, 82.

(50) Tse, Y. C.; Newton, M. D. *J. Am. Chem. Soc.* **1977**, *99*, 611.

(51) Curtiss, L. A. *J. Chem. Phys.* **1977**, *67*, 1144.

(52) Tse, Y. C.; Newton, M. D.; Allen, L. C. *Chem. Phys. Lett.* **1980**, *75*, 350.

(53) Shivaglal, M. C.; Sing, S. *Int. J. Quantum Chem.* **1989**, *36*, 105.

(54) Maes, G.; Smets, J. *J. Phys. Chem.* **1993**, *97*, 1818.

(55) Matsumoto, M.; Takaoka, Y.; Kataoka, Y. *J. Chem. Phys.* **1993**, *98*, 1464.

(56) Wang, J.; Boyd, R. J.; Laaksonen, A. *J. Chem. Phys.* **1996**, *104*, 7261.

(57) Zakharov, V. V.; Brodskya, E. N.; Laaksonen, A. *J. Chem. Phys.* **1998**, *109*, 9487.

(58) Jorgensen, W. L. *J. Phys. Chem.* **1989**, *90*, 1276.

(59) El-Shall, M. S.; Daly, G. M.; Wright, D. *J. Chem. Phys*. **2002**, *116*, 10253.

(60) Jorgensen, W. L.; Severance, D. L. *J. Am. Chem. Soc.* **1990**, *112*, 4768.

(61) Gregory, V. P.; Schug, J. C. *Mol. Phys.* **1993**, *78*, 407.

(62) Losada, M.; Leutwler, S. *J. Chem. Phys.* **2002**, *117*, 2003.

(63) Ludwig, R. *Angew. Chem., Int. Ed.* **2001,** *40*, 1808.

(64) Schmidt, M. W.; Baldridge, K. K.; Boatz, J. A.; Elbert, S. T.; Gordon, M. S.; Jensen, J. J.; Koseki, S.; Matsunaga, N.; Nguyen, K. A.; Su, S.; Windus, T. L.; Dupuis, M.; Montgomery, J. A. *J. Comput. Chem.* **1993**, *14*, 1347.

(65) Jorgensen, W. L.; Laird, E. R.; Nyugen, T. B.; Tirado-Rives, J. *J. Comput. Chem.* **1993**, *14*, 206.

(66) Pitzer, K. S.; Guttman, L.; Westrum, E. F., Jr. *J. Am. Chem. Soc.* **1946**, *68*, 2209.

(67) *Selected Values of Properties of Chemical Compounds*; Thermodynamics Research Center: Texas A&M University, College Station, TX, 1997.

(68) Warfield, R. W.; Petree, M. C. *J. Polym. Sci.* **1961**, *55*, 497.

(69) Lebedev, B. V.; Lebedev, N. K.; Smirnova, N. N.; Kozyreva, N. M.; Kirillin, A. I.; Korshak, V. V. *Dokl. Akad. Nauk, SSSR* **1985**, *281*, 379.

(70) *Hawley's Condensed Chemical Dictionary*, 12th ed.; Van Nostrand Reinhold Company: New York, 1993; p 1097.

(71) Jorgensen, W. L.; Maxwell, D. S.; Tirado-Rives, J. *J. Am. Chem. Soc.* **1996**, *118*, 11225.

(72) Garrett, A. W.; Severance, D. L.; Zwier, T. S. *J. Chem. Phys.* **1992**, *98*, 7245.

(73) Mahmoud, H.; Germanenko, I. N.; Ibrahim, Y.; El-Shall, M. S. *J. Phys. Chem.* **2003**, *107*, 5920.

(74) Bernstein, E. R. In *Atomic and Molecular Clusters*; Bernstein, E. R., Ed.; Elsevier: Amsterdam, 1990.